

Antimonide-based pN terahertz mixer diodes

R. Magno,^{a)} J. G. Champlain, H. S. Newman, and D. Park
Naval Research Laboratory, Washington, DC 20375

(Received 27 October 2010; accepted 11 January 2011; published 3 February 2011)

High frequency pN heterojunction diodes with cutoff frequencies over 1 THz have been fabricated using narrow bandgap high-mobility semiconductors. The pN heterojunction is composed of a 30 nm thick *p*-type $\text{In}_{0.27}\text{Ga}_{0.73}\text{Sb}$ alloy and a 130 nm thick $\text{In}_{0.69}\text{Al}_{0.31}\text{As}_{0.41}\text{Sb}_{0.59}$ *n*-layer. A high-mobility *n*-type $\text{InAs}_{0.66}\text{Sb}_{0.34}$ contact layer is used to connect the mesa diode to a metal Ohmic contact. These alloys have a lattice constant $a_0=6.2$ Å and are grown on semi-insulating GaAs, $a_0=5.65$ Å, using a buffer consisting of 1 μm of $\text{In}_{0.21}\text{Ga}_{0.19}\text{Al}_{0.6}\text{Sb}$ with $a_0=6.2$ Å and 0.5 μm of $\text{Ga}_{0.35}\text{Al}_{0.65}\text{Sb}$ with $a_0=6.12$ Å. © 2011 American Vacuum Society. [DOI: 10.1116/1.3549885]

I. INTRODUCTION

The group of semiconductors consisting of InAs, GaSb, AlSb, and InSb and their ternary and quaternary alloys with lattice constants from that of InAs at 6.058 Å to InSb at 6.479 Å are of interest in the development of high-speed low-power electronics. Several electronic devices using these alloys are under development including the InAs channel high electron mobility transistors, the heterojunction bipolar transistors, the resonant tunneling diodes, and a backward diode for use as a zero-biased detector.¹ Recently, there has been an interest in using these high-mobility narrow bandgap materials to develop a terahertz subharmonic mixer.^{2,3} The nonlinear properties of a subharmonic mixer are used to generate a signal with frequency $\omega_{\text{if}}=\omega_{\text{LO}}-\omega$ by mixing power from a local oscillator at ω_{LO} , with the signal of interest at ω . The goal of this effort is to develop a subharmonic mixer that can operate in the terahertz frequency range that requires little local oscillator power by using molecular beam epitaxy (MBE) to grow thin high-mobility narrow bandgap semiconductors using this material system.

The terahertz subharmonic devices are of interest for applications in imaging systems, in spectroscopic systems for chemical identification, and in communications. Arrays with many mixers would be advantageous in the imaging and spectroscopic applications. Small light-weight systems that could be hand held or carried in an airplane or satellite are highly desired. The development of a mixer that will work with little local oscillator power is useful as there is no high-power light-weight source for use as a local oscillator source at these high frequencies. The use of the high-mobility materials available in this material system also holds the promise of developing higher frequency mixer diodes than those currently available.

The diode's ability to work with low local oscillator power results from using narrow bandgap semiconductors to form a pN heterojunction diode as only a small voltage is needed to drive a forward bias current. Additional power savings result from the reduction in parasitic series resistances, R_s , obtained by using high-mobility semiconductors. The pN diode has been used as it is difficult to form the

Schottky barriers on narrow bandgap semiconductors. This article reports on a pN diode with one particular combination of InGaSb/InAlAsSb semiconductors with a 6.2 Å lattice constant, but by changing the composition it may be possible to make to devices with an even narrower bandgap requiring even lower local oscillator power and with smaller series resistance resulting in lower power dissipation. Going to smaller bandgap higher mobility semiconductors means growing semiconductors with larger lattice constants. How much farther it is possible to go needs to be determined as there may be problems associated with growing materials with an even larger lattice mismatch with the available substrates.

The pN diodes are generally not used as terahertz mixers as the junction may have a large capacitance, C_j , due to the diffusion capacitance when forward biased. The $R_s C_j$ cutoff frequency, $f_{RC}=1/2\pi R_s C_j$, is a measure of the maximum possible frequency. The diffusion capacitance is associated with the diffusion of electrons into the *p*-layer and holes into the *n*-layer when the diode is forward biased. The GaAs Schottky diodes, which have no diffusion capacitance, are frequently used to make high frequency mixer diodes. This article describes several features of the InGaSb/InAlAsSb pN diode that act to minimize the diffusion capacitance and series resistance in order to obtain values of f_{RC} greater than 1 THz.

II. EXPERIMENT

The diodes were grown in a Riber 32P solid-source MBE machine equipped with a reflection high-energy electron diffraction (RHEED) system for monitoring the growths. It also has a system that uses band edge spectroscopy to measure the substrate temperature. Maintaining the substrate temperature is crucial and difficult to do when growing narrow bandgap semiconductors. The narrow bandgap layers absorb energy from the substrate light that passes through the previously deposited layers, and as the layer gets thicker more energy is absorbed. As a result, the substrate temperature will increase unless the power to the substrate heater is reduced to compensate for the additional energy absorption. The system is equipped with valved sources for both As_2 and Sb_2 that are crucial for obtaining the proper Sb and As com-

^{a)}Electronic mail: richard.magno@nrl.navy.mil

positions in the layers containing mixed group V alloys. All the layers were grown as random alloys that required careful calibrations to get the desired compositions particularly for the mixed group V alloys. The starting point for obtaining the proper group III compositions is the measurement of RHEED intensity oscillations while growing GaAs, AlSb, and InAs test structures. Eventually, calibration samples of the individual $\text{In}_{0.27}\text{Ga}_{0.73}\text{Sb}$, $\text{Ga}_{0.35}\text{Al}_{0.65}\text{Sb}$, or $\text{In}_{0.21}\text{Ga}_{0.19}\text{Al}_{0.6}\text{Sb}$ layers are grown and x-ray diffraction measurements are made to check for the proper lattice constant. Assuming the group III elements have a sticking coefficient of 1, test layers of the individual mixed group V alloys $\text{In}_{0.69}\text{Al}_{0.31}\text{As}_{0.41}\text{Sb}_{0.59}$ and $\text{InAs}_{0.66}\text{Sb}_{0.34}$ are grown. X-ray diffraction measurements are made to determine if the layers have the desired lattice constant. Adjustments are made to the As and Sb valve settings to modify the compositions to obtain the desired lattice constant. The precise group III composition is uncertain, and the numbers quoted are obtained by using the interpolation scheme and data given by Vurgaftman *et al.*⁴ Photoluminescence data have been reported for a few of the alloys used here. The PL data confirmed the band alignments and gave a measure of the low temperature bandgaps for the $\text{In}_{0.27}\text{Ga}_{0.73}\text{Sb}/\text{In}_{0.69}\text{Al}_{0.31}\text{As}_{0.41}\text{Sb}_{0.59}$ alloys.⁵ Additional details on the growth of the $\text{In}_{0.27}\text{Ga}_{0.73}\text{Sb}/\text{In}_{0.69}\text{Al}_{0.31}\text{As}_{0.41}\text{Sb}_{0.59}$ alloys have also been published.⁶ Te and Be are used for the *n*-type and *p*-type dopants, respectively. The Hall effect measurements have been made on test layers to determine the proper cell temperatures to obtain the desired carrier concentration for the different alloys.

III. RESULTS AND DISCUSSION

Diodes have been successfully grown on both semi-insulating (SI) GaAs and SI Fe doped InP substrates. The first step for each is a thermal oxide off procedure using an As_2 flux to inhibit the surface from becoming metal rich. Figure 1(a) illustrates that when a GaAs substrate is used 100 nm of GaAs is grown to smooth out any roughness due to the thermal oxide off procedure. A 200 nm thick $\text{In}_{0.52}\text{Al}_{0.48}\text{As}$ layer that is nearly lattice matched to SI InP is grown when an InP substrate is used. This layer provides a transition from a P alloy, InP, to an As alloy.

Several important properties of the pN diode can be understood by examining the band structure of the pN diode that is shown in Fig. 1(b). The 500 meV bandgap of the p^+ $\text{In}_{0.27}\text{Ga}_{0.73}\text{Sb}$ layer sets the size of the voltage necessary to forward bias the diode. This results in the low voltage, thus low-power operation. Even lower voltage operation should be realized by moving to an InGaSb alloy with a larger In fraction. The 500 meV needed for forward bias is an advantage over the GaAs Schottky diode that requires a larger voltage determined by the Schottky barrier height. It should also be noted that the InGaSb is relatively easy to grow as it is not a mixed group V alloy. When forward biased, minority carrier electrons are injected into the *p*-layer and contribute to the diffusion capacitance. The 30 nm thick *p*-layer minimizes the minority carrier electron contribution to the diffu-

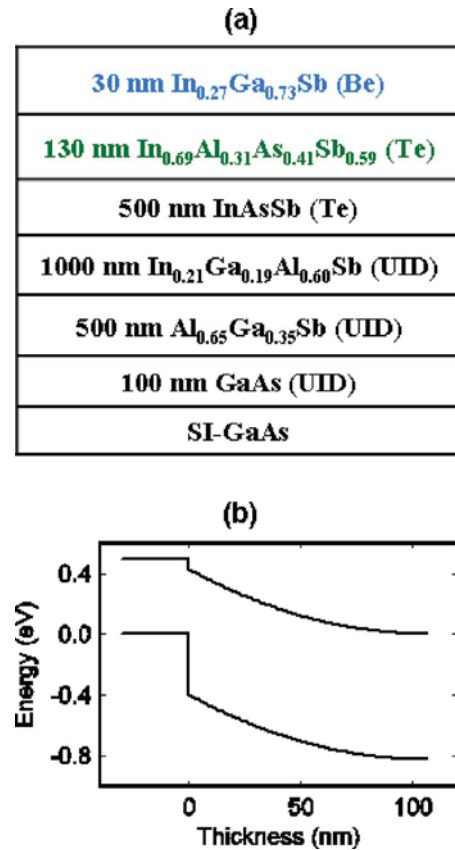


FIG. 1. (Color online) (a) Layer structure of a pN heterojunction grown on SI GaAs substrate, including the unintentionally doped (UID) buffer layers, the $\text{InAs}_{0.66}\text{Sb}_{0.34}$ contact layer, and the *p* and *n* junction layers (b) energy bands at the pN junction indicating the small 0.5 eV band gap of the *p*-layer, the large valence band offset, and the small conduction band offset.

sion capacitance by allowing them to be quickly collected at the *p*-layer Ohmic contact. The valence band offset between $\text{In}_{0.27}\text{Ga}_{0.73}\text{Sb}$ and $\text{In}_{0.69}\text{Al}_{0.31}\text{As}_{0.41}\text{Sb}_{0.59}$ prohibits holes from traveling from the *p*-layer into the *n*-layer, thereby eliminating that contribution to the diffusion capacitance. These structural factors make this pN diode act like a pseudo-Schottky barrier.

An important part of this problem is the development of a suitable buffer layer to accommodate the lattice mismatch between the $\text{In}_{0.69}\text{Al}_{0.31}\text{As}_{0.41}\text{Sb}_{0.59}/\text{In}_{0.27}\text{Ga}_{0.73}\text{Sb}$ layers with a 6.2 Å lattice constant and the substrate lattice constant. A 500 nm $\text{Ga}_{0.35}\text{Al}_{0.65}\text{Sb}$ layer with $a_0=6.12$ Å is grown first and followed by an $\text{In}_{0.21}\text{Ga}_{0.19}\text{Al}_{0.6}\text{Sb}$ layer with $a_0=6.2$ Å. There is some latitude in the composition of both these layers. The $\text{Ga}_{0.35}\text{Al}_{0.65}\text{Sb}$ is grown at a rate of 1 monolayer (ML)/s at a substrate temperature of 500–530 °C. An in-depth study of a similar alloy $\text{Ga}_{0.2}\text{Al}_{0.8}\text{Sb}$ has recently been published.⁷ The $\text{In}_{0.21}\text{Ga}_{0.19}\text{Al}_{0.6}\text{Sb}$ alloy is relatively unknown as there are few growths reported for similar alloys with lattice constants near 6.2 Å. Calculations using the data of Vurgaftman *et al.* gave 1.47 and 1.66 eV for the room temperature direct bandgaps for the $\text{In}_{0.21}\text{Ga}_{0.19}\text{Al}_{0.6}\text{Sb}$ and $\text{Ga}_{0.35}\text{Al}_{0.65}\text{Sb}$ alloys, respectively. The change in composition results in a slight reduction in a reasonably large band-

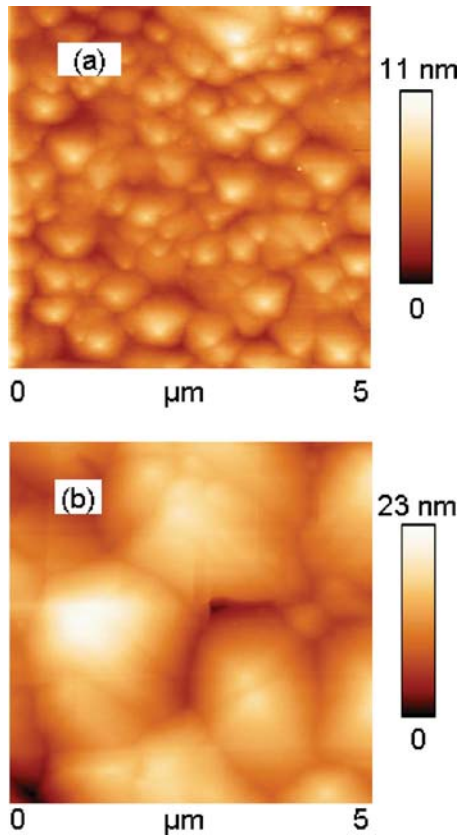


FIG. 2. (Color online) Atomic force microscope images and color bars for the surfaces of (a) $\text{Ga}_{0.35}\text{Al}_{0.65}\text{Sb}$ with an rms=1.2 nm and P - V =11 nm and (b) $\text{In}_{0.21}\text{Ga}_{0.19}\text{Al}_{0.6}\text{Sb}$ with an rms=3.6 nm and P - V =23 nm.

gap. The valence band offsets were also calculated and found to be nearly the same at 240 meV for the $\text{In}_{0.21}\text{Ga}_{0.19}\text{Al}_{0.6}\text{Sb}$ and 260 meV for the $\text{Ga}_{0.35}\text{Al}_{0.65}\text{Sb}$. Many of the parameters involved in the $\text{In}_{0.21}\text{Ga}_{0.19}\text{Al}_{0.6}\text{Sb}$ growth have not been thoroughly explored. The layers used here were grown at a substrate temperature of 470 °C. A ten period, short period, superlattice, each period consisting of 5 ML of $\text{In}_{0.26}\text{Al}_{0.74}\text{Sb}$ and 5 ML of $\text{Ga}_{0.24}\text{Al}_{0.76}\text{Sb}$, was grown first to aid in the transition from the 6.12 Å $\text{Ga}_{0.35}\text{Al}_{0.65}\text{Sb}$ layer. Atomic force microscopy (AFM) was used to measure the surface topography for typical layers of $\text{Ga}_{0.35}\text{Al}_{0.65}\text{Sb}$ [Fig. 2(a)] and $\text{In}_{0.21}\text{Ga}_{0.19}\text{Al}_{0.6}\text{Sb}$ [Fig. 2(b)]. Both images show islandlike features that are randomly distributed and isotropic with no favored lattice orientation. The sizes of the features in the AFM images increase, suggesting that as the layers get thicker the islands coalesce suggesting a reduction in the dislocations on going from the $\text{Ga}_{0.35}\text{Al}_{0.65}\text{Sb}$ surface to the $\text{In}_{0.21}\text{Ga}_{0.19}\text{Al}_{0.6}\text{Sb}$ top surface. The AFM rms roughness and peak-to-valley P - V ratios of 1.2 and 11 nm, respectively, for the $\text{Ga}_{0.35}\text{Al}_{0.65}\text{Sb}$ are found to increase on going to the $\text{In}_{0.21}\text{Ga}_{0.19}\text{Al}_{0.6}\text{Sb}$ alloy. The $\text{In}_{0.21}\text{Ga}_{0.19}\text{Al}_{0.6}\text{Sb}$ in Fig. 2(b) has AFM rms roughness of 3.6 nm and a P - V of 23 nm that is typical of many growths. The best rms roughness and P - V values obtained to date for this alloy are 2.4 and 14 nm, respectively, so it is possible to do much better.

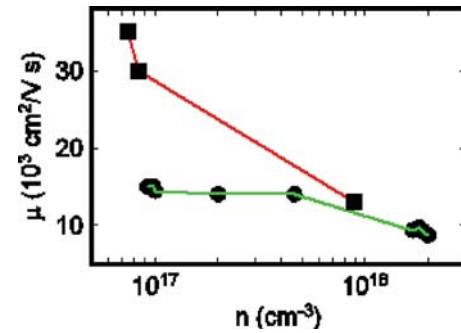


FIG. 3. (Color online) Comparison of the mobility, μ , vs electron concentration, n , for $\text{InAs}_{0.66}\text{Sb}_{0.34}$ grown on $\text{Ga}_{0.35}\text{Al}_{0.65}\text{Sb}$ with $a_0=6.12$ Å (circles) and $\text{In}_{0.21}\text{Ga}_{0.19}\text{Al}_{0.6}\text{Sb}$ with $a_0=6.2$ Å (squares). The lines are included as a guide for the eyes.

The value of using the $\text{In}_{0.21}\text{Ga}_{0.19}\text{Al}_{0.6}\text{Sb}$ layer is demonstrated by examining Fig. 3 that contains the Hall effect data obtained for the 500 nm thick $\text{InAs}_{0.66}\text{Sb}_{0.34}$ with $a_0=6.2$ Å that were grown at a substrate temperature of 430 °C at a rate of 0.5 ML/s. This is the alloy used for the contact layer in Fig. 1(a). The data points represented by the circles were obtained for $\text{InAs}_{0.66}\text{Sb}_{0.34}$ grown on the 6.12 Å $\text{Ga}_{0.35}\text{Al}_{0.65}\text{Sb}$ buffer layer, while the points represented by the squares were obtained for layers grown on the 6.2 Å $\text{In}_{0.21}\text{Ga}_{0.19}\text{Al}_{0.6}\text{Sb}$ buffer. The lines connecting the points are included as a guide for the eyes. The mobility for the UIDs on $\text{In}_{0.21}\text{Ga}_{0.19}\text{Al}_{0.6}\text{Sb}$ reached 35 000 $\text{cm}^2/\text{V s}$ compared to 15 000 $\text{cm}^2/\text{V s}$ for those on the $\text{Ga}_{0.35}\text{Al}_{0.65}\text{Sb}$ buffer. A slightly lower electron concentration of $7.5 \times 10^{16} \text{ cm}^{-3}$ compared to $9.5 \times 10^{16} \text{ cm}^{-3}$ is found for the 35 000 $\text{cm}^2/\text{V s}$ layer compared to the 15 000 $\text{cm}^2/\text{V s}$ layer. Mobility calculations for this composition predict that without dislocations the mobility should be near 57 000 $\text{cm}^2/\text{V s}$.⁸ These results suggest that dislocation scattering is important in determining the $\text{InAs}_{0.66}\text{Sb}_{0.34}$ mobility. The mobility of 35 000 $\text{cm}^2/\text{V s}$ reported here should be compared with other reports in the literature for InAsSb with similar compositions. Coderre and Woolley in 1968 reported a mobility of 22 000 $\text{cm}^2/\text{V s}$ for a bulk sample of $\text{InAs}_{0.64}\text{Sb}_{0.36}$.⁹ More recently, a value of 11 000 $\text{cm}^2/\text{V s}$ for an $\text{InAs}_{0.5}\text{Sb}_{0.5}$ alloy was reported in a paper that compared the effectiveness of other buffers when growing $\text{InAs}_x\text{Sb}_{1-x}$ on GaAs.¹⁰

The average AFM rms roughness and P - V for a group of the $\text{InAs}_{0.66}\text{Sb}_{0.34}$ layers are similar to the average AFM data for a group of $\text{In}_{0.21}\text{Ga}_{0.19}\text{Al}_{0.6}\text{Sb}$ layers indicating that little surface degradation takes place when $\text{InAs}_{0.66}\text{Sb}_{0.34}$ is grown on $\text{In}_{0.21}\text{Ga}_{0.19}\text{Al}_{0.6}\text{Sb}$.

The x-ray data also indicate a reduction in the dislocations as the full width at half maximum decreased from 674 to 473 arc sec when the $\text{In}_{0.21}\text{Ga}_{0.19}\text{Al}_{0.6}\text{Sb}$ buffer is used. It should also be mentioned that only one peak is found in the x ray for $\text{InAs}_{0.66}\text{Sb}_{0.34}$, indicating that there is no evidence for phase separation.

A low resistance contact layer is important as it connects the diode mesa to the *n*-layer metal Ohmic contact. This is about 2 μm with the current lithography and can add substantially to the series resistance. The $\text{InAs}_{0.66}\text{Sb}_{0.34}$ contact layer has several advantages over the $\text{In}_{0.27}\text{Ga}_{0.73}\text{Sb}$ contact layer reported for a previously reported pN diode.¹¹ The new $\text{InAs}_{0.66}\text{Sb}_{0.34}$ layer doped with Te to a carrier concentration of $3 \times 10^{18} \text{ cm}^{-3}$ and has a Hall mobility of $5600 \text{ cm}^2/\text{V s}$ and a contact resistance of $2.4 \times 10^{-8} \Omega \text{ cm}^2$.¹¹ These numbers are significantly better than the mobility of $4500 \text{ cm}^2/\text{V s}$ and contact resistance of $2.5 \times 10^{-5} \Omega \text{ cm}^2$ for $\text{In}_{0.27}\text{Ga}_{0.73}\text{Sb}$ contact layer. The average values for AFM rms roughness and *P-V* for a group of $\text{InAs}_{0.66}\text{Sb}_{0.34}$ layers are 3.3 and 22 nm, respectively. These numbers indicate that it is smoother than the $\text{In}_{0.27}\text{Ga}_{0.73}\text{Sb}$ used earlier that had an average rms roughness of 4 nm and *P-V* of 33 nm. The cost to using the $\text{InAs}_{0.66}\text{Sb}_{0.34}$ is that a mixed group V alloy is somewhat more difficult to grow than a mixed group III alloy. The completed pN diode typically has a rms roughness between 3.6 and 4 and a *P-V* ranging from 22 to 28, indicating that a small amount of additional roughness occurs during the growth of the pN layers.

High frequency operation also requires the ability of the electrons injected into the *p*-type $\text{In}_{0.27}\text{Ga}_{0.73}\text{Sb}$ to be rapidly removed from it. To enhance this possibility a very thin, 30 nm thick, *p*-layer has been used. A minority carrier electron will either transit the layer and be removed at the metal/ $\text{In}_{0.27}\text{Ga}_{0.73}\text{Sb}$ *p*-type Ohmic contact or it will recombine with a hole injected at that contact. The holes supplied at the Ohmic contact are expected to experience a very low resistance. Prior measurements have reported very low contact resistances of $7.6 \times 10^{-8} \Omega \text{ cm}^{-2}$ for $\text{In}_{0.27}\text{Ga}_{0.73}\text{Sb}$ with hole concentrations of $3 \times 10^{19} \text{ cm}^{-3}$.¹² A very low resistance of $2 \times 10^{-2} \Omega$ is calculated for a $2 \times 5 \mu\text{m}^2$ 30 nm thick mesa using the high hole mobilities of $160 \text{ cm}^2/\text{V s}$ reported for this semiconductor.⁶ The very small indium concentration, 0.27, suggests that the alloy is similar to GaSb that has the Fermi level at the surface pinned near the valence band. This suggests that the electrons diffusing across the $\text{In}_{0.27}\text{Ga}_{0.73}\text{Sb}$ also have a small barrier height at the Ohmic contact leading to a low contact resistance. The resistance they experience in the *p*-type is uncertain, but the electron mobilities in *n*-type $\text{In}_{0.27}\text{Ga}_{0.73}\text{Sb}$ are at least ten times larger than the hole mobilities.

An effort has been made to determine the high frequency performance of the pN diode by fabricating devices with ground-signal-ground leads suitable for connecting to a network analyzer operating from 10 MHz to 50 GHz. Short circuit and open circuit standards were also fabricated on the same wafer to obtain data to de-embed the diode from the transmission line parasitics. The de-embedded data were fit to a lumped-element equivalent circuit consisting of a resistance R_s in series with a shunt junction capacitance-conductance pair. The results indicate that R_s is very small compared to the 50 Ω characteristic impedance that the reflection coefficient is normalized against. The preliminary results are illustrated in Fig. 4 where the area dependence of

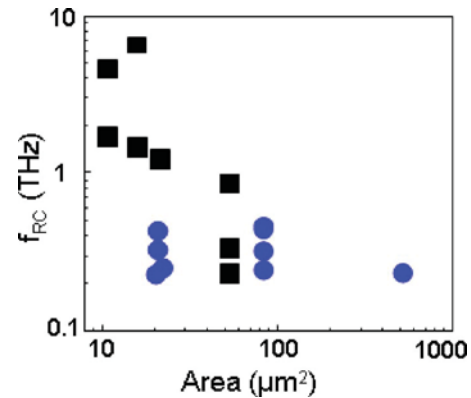


FIG. 4. (Color online) Cutoff frequency, f_{RC} , for several circular and rectangular shaped pN diodes with several different areas.

the cutoff frequency for several circular and rectangular diodes is presented. The frequency of the circular diodes is independent of the area for the contact geometry used here, while the frequency of the rectangular diodes increases as the area is reduced. The small area rectangular diodes that indicate cutoff frequencies over a terahertz are possible. The area dependence of the rectangular diodes suggests that higher frequencies may be obtained with improved device geometry. The difficulty with this measurement is tied to achieving the goal of making a pN mixer diode with a small capacitance using narrow bandgap high-mobility semiconductors. Higher frequency tests are planned to obtain more accurate measurements of the properties of these diodes.

IV. SUMMARY AND CONCLUSIONS

An important result of this work is that by using high-mobility narrow bandgap semiconductors with the appropriate valence, conduction band offsets, and thin layers it is possible to make pN heterojunction diodes with cutoff frequencies above a terahertz. Many changes can be made to produce diodes with even higher operating frequencies and lower local oscillator power requirements. Chief among the material changes is to move to an alloy set with higher indium content. At $a_0=6.3 \text{ \AA}$ the *p*-layer would have a composition of $\text{In}_{0.53}\text{Ga}_{0.47}\text{Sb}$ and a bandgap of 0.33 eV resulting in a power savings. The electron mobility in this alloy is expected to approach that of InSb leading to a faster diffusion of the electron minority carriers across the *p*-layer. The composition of the *n*-layer would be something like $\text{In}_{0.83}\text{Al}_{0.17}\text{As}_{0.28}\text{Sb}_{0.72}$ that would also be expected to have a higher electron mobility approaching that of InSb. The current alloy, $\text{In}_{0.69}\text{Al}_{0.31}\text{As}_{0.41}\text{Sb}_{0.59}$, has a mobility of $2700 \text{ cm}^2/\text{V s}$ which is the lowest of the alloys used in the present device. The layer thicknesses and doping of the current diode as well as the planar geometry of the diode/contacts can also be adjusted to enhance its performance.

The $\text{InAs}_{0.66}\text{Sb}_{0.34}$ mobility data point to the importance of improving the buffer layers to reduce the dislocations that act to reduce carrier mobilities. Improvements in the morphology are also expected to be important as the lateral di-

mensions of the diodes shrink. As mentioned the best AFM roughness of the $\text{Ga}_{0.35}\text{Al}_{0.65}\text{Sb}/\text{In}_{0.21}\text{Ga}_{0.19}\text{Al}_{0.6}\text{Sb}$ obtained so far is better than the average found for a number of test structures indicating that improvements are possible. The ability to move to diodes with a lattice constant approaching 6.3 \AA depends on the ability to build a suitable buffer layer. An additional restraint may be that as the lateral diode dimensions shrink the lithographic processes require thinner buffers between the diode and the semi-insulating substrate.

ACKNOWLEDGMENT

This work was supported by the Office of Naval Research.

¹B. R. Bennett, R. Magno, J. B. Boos, W. Kruppa, and M. G. Ancona, *Solid-State Electron.* **49**, 1875 (2005).

²J. G. Champlain, R. Magno, D. Park, H. S. Newman, and J. B. Boos, in *Conference Digest of the 2007 Joint 32nd International Conference on Infrared and Millimeter Waves and the 15th International Conference on*

Terahertz Electronics, edited by M. J. Griffin, P. C. Hargrove, T. J. Parker, and K. P. Wood (IEEE, Piscataway, NJ, 2007), pp. 855 and 856.

³R. Magno, J. G. Champlain, H. S. Newman, M. G. Ancona, J. C. Culbertson, B. R. Bennett, J. B. Boos, and D. Park, *Appl. Phys. Lett.* **92**, 243502 (2008).

⁴I. Vurgaftman, J. R. Meyer, and L. R. Ram-Mohan, *J. Appl. Phys.* **89**, 5815 (2001).

⁵E. R. Glaser, R. Magno, B. V. Shanabrook, and J. G. Tischler, *Phys. Rev. B* **74**, 235306 (2006).

⁶R. Magno, E. R. Glaser, B. P. Tinkham, J. G. Champlain, J. B. Boos, M. G. Ancona, and P. M. Campbell, *J. Vac. Sci. Technol. B* **24**, 1622 (2006).

⁷B. R. Bennett, S. A. Khan, J. B. Boos, N. A. Papanicolaou, and V. V. Kuznetsov, *J. Electron. Mater.* **39**, 2196 (2010).

⁸D. Chattopadhyay, S. K. Sutradhar, and B. R. Nag, *J. Phys. C* **14**, 891 (1981).

⁹W. M. Coderre and J. C. Woolley, *Can. J. Phys.* **46**, 1207 (1968).

¹⁰S. Nakamura, P. Jayavel, T. Koyama, and Y. Hayakawa, *J. Cryst. Growth* **300**, 497 (2007).

¹¹J. G. Champlain, R. Magno, and J. B. Boos, *Electron. Lett.* **43**, 1315 (2007).

¹²J. G. Champlain, R. Magno, and J. B. Boos, *J. Vac. Sci. Technol. B* **24**, 2388 (2006).